MAINE Flow facility for the measurement of liner properties in presence of multi-modal acoustic field and grazing flow: Qualification and first liner characterization

Joachim Golliard
CTTM Le Mans, 20 rue Thalès de Milet, 72000 Le Mans, France
LAUM, Le Mans Université, France

Thomas Humbert
Laboratoire d'Acoustique de l'Université du Mans (LAUM) UMR CNRS 6613, Le Mans Université, Avenue Olivier Messiaen, 72085 Le Mans Cedex 9, France

Jean-Christophe Le Roux, Eric Portier
CTTM Le Mans, 20 rue Thalès de Milet, 72000 Le Mans, France

This paper reports the qualification measurements of a test rig built by Le Mans Université to investigate the acoustic properties of liners in flow and acoustic conditions typically found in nacelles of aircraft engines. The facility is called MAINE Flow, for Multimodal Acoustic ImpedaNce Eduction with Flow. Typically, liners used to reduce engine noise emissions are characterized by their acoustic impedance, which can be computed from empirical or (semi-)analytical models or measured to account for the effects of flow. Propagation codes are then used to predict the effect of the liner installation on the radiated noise.

The concept of impedance is well-defined without flow, but is not uniquely defined in presence of flow. On relatively small test-rigs, differences have been observed in presence of grazing flow between the impedance measured for acoustic plane waves traveling in direction of the flow and in the opposite direction. An objective of the new, larger, test-rig is to investigate if these differences are also observed for propagating modes beyond the plane wave. Therefore, an important characteristic of the new test-rig is that it can measure the acoustic properties for different acoustic modes independently of each other. Furthermore, it can be used to qualify liners and innovative acoustic treatments in flow and acoustic conditions close to flight conditions and thereby asses their maturity.

The tests reported here focus on: the modal decomposition of the acoustic field, the way a specific mode or a combination of modes are excited by the system of acoustic sources, the measurement of the multi-modal scattering matrix. When possible, the qualification was performed without flow and with flow up to M=0.6.

I. Introduction

Le Mans Université has built a test-rig for investigating acoustic properties of liners in flow and acoustic conditions typically found in nacelles of aircraft engines. The facility is called MAINE Flow, for Multimodal Acoustic ImpedaNce Eduction with Flow and its general characteristics were described in [1]. The liners used in aeronautics to reduce noise emissions are typically characterized by their acoustic impedance, which can be computed from empirical or (semi-)analytical models or measured to account for the flow effects. Propagation codes are then used to predict the effect of the liner on the radiated noise. Whereas the concept of impedance is well-defined without flow, it is not uniquely defined in presence of flow. In particular, it has been shown on smaller test rigs that the impedance measured when the acoustic plane waves propagate in the same direction as the flow is different from the one found when they travel in the opposite direction [2–4]. An objective of the larger test-rig presented here is to investigate if these differences are also observed for propagating modes beyond the plane wave. Therefore, an important characteristic of the facility is that it can measure the acoustic liner properties for different acoustic modes independently of each other. Furthermore, it can be used to qualify liners and innovative acoustic treatments in flow and acoustic conditions which are close to flight conditions and thereby asses their maturity for use in real conditions. Indeed, since the liner sample is installed flush in a

150 x 280 mm^2 rectangular duct, the height of the duct in the direction that faces the test sample (280 mm) is close to the free space facing the liner in an aircraft engine nacelle, particularly in the annular by-pass duct. Furthermore, the liner can be subjected to a grazing flow with a mean Mach number up to M=0.6 and to an incident acoustic field up to 150 dB.

II. Structure and functionalities of the test rig

The general characteristics of the installation were described [1] and are briefly reminded here. The main part of the test rig consists of a 10 m long rectangular duct (280 mm x 150 mm) where the liner sample is mounted on one of the small sides, in the center. Furthermore, loudspeakers and compression chambers are mounted on each side of the sample to create the multimodal acoustic field. Between the sources and the test sample, microphones have been mounted to measure (and control) this field.

The flow is generated by a fan used in suction mode and separated from the test section by a diverging section and mufflers. The temperature at the test section is controlled and kept constant with a heating section located in the settling chamber upstream of the convergent where air gets in at atmospheric conditions.

In order to reproduce flow conditions representative of the inlet of an aircraft engine, it was decided that the test-rig should be able to operate at a flow velocity up to M = 0.6 in the test section where the liner sample is located. The other main requirement was that an acoustic field characteristic of the inlet section of an aircraft engine can be reproduced. There, and due to the strong rotational nature of the excitation (rotating blades of the fan), circumferential modes are dominant. Since it is simpler to produce and equip a rectangular test section than a circular (or annular) one (and also to produce flat liner samples than curved liner samples), the test section (where the liner will be characterized) is rectangular with a cross-section of 280 mm x 150 mm. The liner sample is placed on the small side. As far as the liner is concerned, the incidence of circumferential modes can be reproduced by transverse modes along the small dimension of the duct. An additional requirement for the acoustic field is that the sound pressure levels should correspond to the levels observed in the inlet section of the nacelle. Thus, a target sound power level of 145 dB has been set for each mode in the range 300 Hz - 5 kHz. Furthermore, a target of 150 dB in broadband noise (without modal control) is set.

For the characterization of the acoustic treatments, the objective is to measure how they scatter an incident acoustic field. This can be done at different levels, from the rather global evaluation of the Insertion Loss (IL) associated with its installation in the duct, to the measurement of the attenuation or the reflection of particular acoustic modes or the assessment of the full (multi-modal) scattering matrix. Therefore, depending on the desired level of analysis, different functionalities are required. For the lower level of analysis, one is interested in a global acoustic power which is injected

Fig. 1 General view of the test duct of the experimental facility.

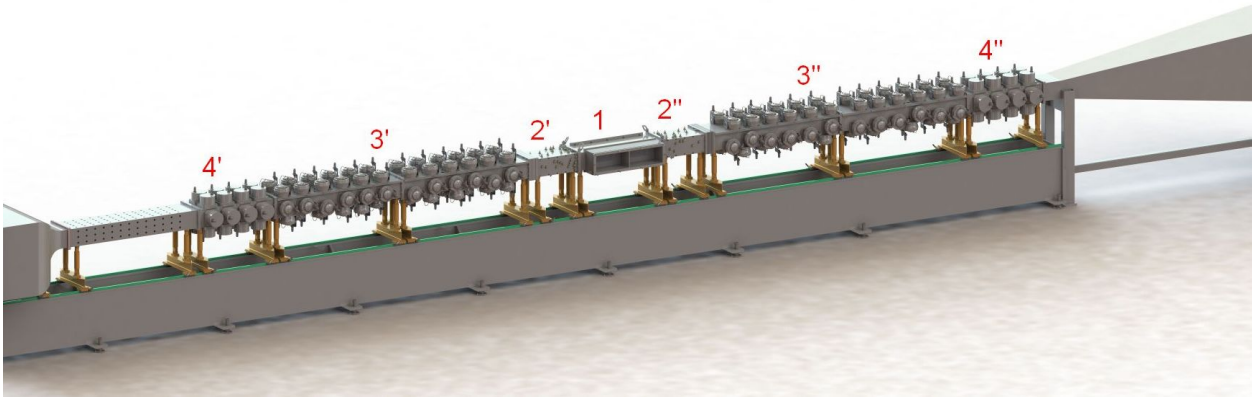

Fig. 2 General view of the test section with (1) the sample support, (2' and 2") the upstream and downstream microphone sections, (3' and 3") the upstream and downstream HF-loudspeaker sections and (4' and 4") the upstream and downstream LF-loudspeaker sections.

on one side of the sample and transmitted on the other side. On the other hand, to measure the multi-modal scattering matrix of the duct with the sample, one needs a number of independent measurements such as a multi-load [5] or a multi-source analysis [6]. Another approach, somewhere in the middle, is to send an acoustic field with a given modal content (similar to the modal content of the application) on the treatment and to measure the scattering of this particular field [7]. In the last two approaches, a reliable decomposition of the acoustic fields on each side of the sample is necessary.

For the generation of a desired acoustic field, the transfer matrix between the signal sent to the sources and the acoustic modes incident on the treatment should be known. This transfer matrix, which depends on the flow velocity and in a lesser way on the temperature, is identified experimentally by a preliminary series of measurements, where each source is excited one after the other. The experimental identification allows to account for any differences which can exist in the performances of the actual sources, including for example the amplifier, the acoustic coupling between each source and the main duct or the exact position of each source.

Therefore, the following basic functions of the test-rig have been implemented and validated, both without flow and with flow:

- Generation of a stepped-sine signal by each source located upstream or downstream of the test sample and simultaneous acquisition by all the microphones located in the upstream and downstream measurement sections;
- Generation of a broadband uncorrelated signal by all the sources located upstream or downstream and simultaneous acquisition by all the microphones located in the upstream and downstream measurement sections;
- Modal decomposition of the acoustic field in the ducts upstream and downstream for both broadband noise and stepped sine sweep cases;
- Identification of the transfer matrix between the acoustic sources and the incident acoustic modes in the duct.

These basic functions then allow to perform the more advanced functions, also without and with flow :

- Measurement of the multi-modal scattering matrix of the duct containing the sample. In theory, once this operation is performed, all the low-level information, such as the IL for random modes or for given mode combinations, can be calculated from this matrix [8]. Furthermore, this is the starting point to determine the (possibly mode-dependent) impedance of the sample using an indirect method, as it is done when only plane waves are present in the duct in smaller test rigs [9].
- Excitation of particular acoustic modes or mode combinations. This operation is based on a pseudo-inversion of the transfer matrix between the sources and the modes, including a penalization to ensure that no source is excited above a certain limit so that the physical integrity of all the sources is preserved;

III. Theory and methods

A. Mode propagation in the duct

The acoustic field in the duct at a given frequency is described as the superposition of a finite number of modes. The acoustic pressures p_j at the positions $\mathbf{x}_j = (x_j, y_j, z_j)$ of the microphones are written as the sum of the contributions of the individual modes. This is done in matrix form using the propagation matrix $\mathbf{M}$ that relates the acoustic pressures p_j at a given set of M positions $\mathbf{x}_j$ to the amplitudes of the $2N$ modes $p_i^{\pm}$:

$$\mathbf{p}(\omega) = \mathbf{M}(\omega)\mathbf{p}^{\pm}(\omega). \tag{1}$$

$\mathbf{p}$ is a vector containing the pressures at the M positions and $\mathbf{p}^{\pm}$ is a vector containing the amplitudes of the N forward-propagating and the N backward-propagating modes:

$$\mathbf{p} = \begin{pmatrix} p_1 \\ p_2 \\ \vdots \\ p_M \end{pmatrix} \quad \text{and} \quad \mathbf{p}^{\pm} = \begin{pmatrix} p_1^+ \\ p_2^+ \\ \vdots \\ p_N^+ \\ p_1^- \\ p_2^- \\ \vdots \\ p_N^- \end{pmatrix}.$$

The propagation matrix $\mathbf{M}$ is expressed here as

$$\mathbf{M} = \begin{bmatrix} \Psi_{1,1}T_{1,1}^+ & \dots & \Psi_{1,N}T_{1,N}^+ & \Psi_{1,1}T_{1,1}^- & \dots & \Psi_{1,N}T_{1,N}^- \\ \vdots & \ddots & \vdots & \vdots & \ddots & \vdots \\ \Psi_{M,1}T_{M,1}^+ & \dots & \Psi_{M,N}T_{M,N}^+ & \Psi_{M,1}T_{M,1}^- & \dots & \Psi_{M,N}T_{M,N}^- \end{bmatrix},$$

with $\Psi_{j,i}$ the shape function of the mode i evaluated at the position x_j and $T_{j,i}^{\pm} = e^{-jk_i^{\pm}x_j}$ describing the axial propagation of the mode i in the positive ($T_{j,i}^+$) or in the negative ($T_{j,i}^-$) direction between the reference position at $x = 0$ and the section of axial position x_j. The axial wave number depends on the Mach number M and on the propagation direction. It is evaluated using the assumption of non-dissipative propagation in a uniform flow as $k_i^{\pm} = \frac{\omega}{c}\frac{M \pm \sqrt{1-\left(\frac{\kappa_i c}{\omega}\right)^2(1-M^2)}}{1-M^2}$, where κ_i is the transverse wave number for mode i.

For a rectangular duct of width W and height H (with the origin of the axes in a corner of the duct), the shape function is $\Psi_{j,i} = cos\left(\frac{n_i \pi y_j}{W}\right) cos\left(\frac{m_i \pi z_j}{H}\right)$ with n_i and m_i the order of mode i along directions y and z and the transverse wave number is expressed as $\kappa_i^2 = \left(\frac{n_i \pi y_j}{W}\right)^2 + \left(\frac{m_i \pi z_j}{H}\right)^2$.

The modes do not need to be sorted in any particular order for this description of the acoustic field. However, to facilitate the administration, they are ordered by increasing cut-on frequency. That is, when the analysis is done for increasing frequencies, the propagation matrix $\mathbf{M}$ has an increasing number of columns, but its first N' columns still correspond to the same modes which were present at a lower frequency.

As described in [1] the positions of the microphones were chosen such that the propagation matrix is well conditioned at all frequencies. This allows a good decomposition of the acoustic field by inversion of the propagation matrix. In general, the number of microphones is larger than the number of propagating modes (except in the highest frequency range). The system is thus over-determined and the inversion is actually a least-square estimation of the solution.

B. Identification of the transfer matrix between sources and modes

It is possible to measure the modes generated by a given source (or combination of sources) by decomposition (as discussed above) of the signals measured by the microphones. In order to generate a given set of modes, it is actually more interesting to evaluate the transfer function between the signal sent to each source and each of the propagating

incident modes present in the duct at a given frequency. Naturally, evaluating the transfer function occurs in two steps, one of which is indeed a measurement, and the other one actually a calculation, as it involves the inversion of the propagation matrix. By doing this for each of the sources located upstream one-by-one, the transfer matrix between the commands sent to the upstream sources and the modes incident on the sample from upstream can be identified:

$$\mathbf{p}_u^+ = \mathbf{H}_u \mathbf{c}_u, \tag{2}$$

with $\mathbf{c}_u$ a vector containing the commands sent to the N_{chn} upstream source channels.

The same operation is done for the downstream sources to provide the transfer matrix between the commands sent to the downstream sources and the modes incident on the sample from downstream:

$$\mathbf{p}_d^- = \mathbf{H}_d \mathbf{c}_d. \tag{3}$$

These transfer matrices $\mathbf{H}_u$ and $\mathbf{H}_d$ depend on the flow velocity and in a lesser way on the temperature. Since they are identified experimentally, it is not necessary to know the exact coupling between each source and the duct or the exact position of the effective acoustic center of each source. Furthermore, if any other factor influences the individual performances of the sources, such as the amplifiers, this is also accounted for implicitly in the identified transfer matrix.

C. Measurement of the scattering matrix

The scattering matrix relates the amplitude of the waves scattered by an element to the amplitude of the incident waves. In case N modes are cut-on in the duct, the scattering matrix $\mathbf{S}$ has dimension $2N \times 2N$:

$$\mathbf{p}_{out} = \mathbf{S} \cdot \mathbf{p}_{in}, \tag{4}$$

with

$$\mathbf{p}_{in} = \begin{pmatrix} \mathbf{p}_u^+ \\ \mathbf{p}_d^- \end{pmatrix}, \mathbf{p}_{out} = \begin{pmatrix} \mathbf{p}_u^- \\ \mathbf{p}_d^+ \end{pmatrix} \text{ and } \mathbf{S} = \begin{bmatrix} \mathbf{R}^+ & \mathbf{T}^- \\ \mathbf{T}^+ & \mathbf{R}^- \end{bmatrix}, \tag{5}$$

where:

- $\mathbf{p}_u^+$ and $\mathbf{p}_d^-$ are the waves incident on the test section, traveling respectively in positive direction (same direction as the flow) in the upstream duct and in negative direction in the downstream duct;
- $\mathbf{p}_u^-$ and $\mathbf{p}_d^+$ are the waves coming from the test section, traveling respectively in positive direction in the downstream duct and in negative direction in the upstream duct;
- $\mathbf{R}^+$ and $\mathbf{R}^-$ are the matrices containing the reflection coefficients for the upstream and downstream waves;
- $\mathbf{T}^+$ and $\mathbf{T}^-$ are the matrices containing the transmission coefficients from upstream to downstream and from downstream to upstream.

This $2N \times 2N$ scattering matrix can be identified using a number n_e (which should be greater than $2N$) of independent excitation cases. Each realization with a given excitation case provides new relation $\mathbf{p}_{out} = \mathbf{S} \cdot \mathbf{p}_{in}$. These n_e realizations are combined in matrix form as:

$$\left[\begin{pmatrix} \mathbf{p}_u^- \\ \mathbf{p}_d^+ \end{pmatrix}_1 \begin{pmatrix} \mathbf{p}_u^- \\ \mathbf{p}_d^+ \end{pmatrix}_2 \cdots \begin{pmatrix} \mathbf{p}_u^- \\ \mathbf{p}_d^+ \end{pmatrix}_{n_e} \right] = \begin{bmatrix} \mathbf{R}^+ & \mathbf{T}^- \\ \mathbf{T}^+ & \mathbf{R}^- \end{bmatrix} \cdot \left[\begin{pmatrix} \mathbf{p}_u^+ \\ \mathbf{p}_d^- \end{pmatrix}_1 \begin{pmatrix} \mathbf{p}_u^+ \\ \mathbf{p}_d^- \end{pmatrix}_2 \cdots \begin{pmatrix} \mathbf{p}_u^+ \\ \mathbf{p}_d^- \end{pmatrix}_{n_e} \right]. \tag{6}$$

In practice, the excitation cases are provided by sending a unit signal to each of the 70 upstream source channels and 70 downstream source channels. The measurements are actually the same as the measurements performed for the identification of the upstream and downstream transfer matrices $\mathbf{H}_u$ and $\mathbf{H}_d$. The system is thus over-determined ($n_e = 2 * 70 > 2N$ for all the frequency range of interest) and it is solved by a least-square estimation.

D. Excitation of particular acoustic modes or mode combinations

In order to reproduce an acoustic field similar to the one found in a real engine, it is necessary to send commands to the sources which create the desired incident modes on the sample. In other words, in order to obtain a given incident sound field, for example from upstream, $\mathbf{p}_u^+$, one should calculate the corresponding commands $\mathbf{c}_u$ for the upstream source channels. This is done by performing a pseudo-inversion of the transfer matrix $\mathbf{H}_u$ (equation 2). This pseudo inversion is done using a penalization technique to ensure that no source is excited above a certain limit, in order to maintain the physical integrity of all the sources.

IV. Experimental results

A. Results for canonical geometries

1. Rigid plate closing the duct

To verify that the identification of the different duct modes present at different frequencies is performed with sufficient accuracy, the matrix of reflection coefficients of a rigid plate closing the duct has been measured. The plate was mounted perpendicular to the axis of the duct in order to offer a good reference for the reflection coefficients: each incident mode should be reflected with the same amplitude and should not excite other modes after reflection ($|R_{ij}| = 1$ for $i = j$ and $|R_{ij}| = 0$ for $i \neq j$). The actual measurement is a reduced case of the measurement procedure described in section III-C to estimate the multi-modal scattering matrix. The rigid plate is installed in place of the sample-carrying section, some upstream source channels are excited one by one, and the measurements are done with upstream microphones only. In Figure 3, the reflection coefficients for the first 4 modes is presented. Note that the complete matrix was solved for each frequency, up to 13 modes at the maximum frequency of 3000 Hz presented here. Except at frequencies close to the cut-on frequencies of the modes, the reflection coefficients on the diagonal are close to 1 (within 0.5% for the plane wave and with 1% for the other modes showed here below 2000 Hz) and the reflection coefficients out of the diagonal are close to 0. At higher frequencies, the reflection coefficients on the diagonal deviate from 1 for two reasons: the number of independent source configurations is limited for this measurements done in an early stage of the development of the facility, which reduces the over-determination at high frequencies, and the visco-thermal attenuation is not taken into account in the propagation wavenumbers.

This measurement shows that the decomposition of the acoustic field without flow can be performed efficiently and that the measurement of the multi-modal reflection matrix with the multiple-source method corresponds to what is expected.

2. Reflection matrix of the anechoic termination

An element of the test-rig which can be important for some of the measurements is the anechoic termination, which is installed upstream of the test duct, just downstream of the nozzle which accelerates the flow. Thus, the reflection matrix of this termination was also measured for its qualification. The results of these measurements, performed with 14 independent acoustic excitation cases, are presented in Figure 4. The reflections are close to 0, both for the reflections of each mode in itself (on the diagonal) as for the diffraction to other modes. Note that these results are less accurate than with the rigid plate, since this measurement was performed with a lower number of excitation cases, not providing additional accuracy brought by the over determination of the system to be solved.

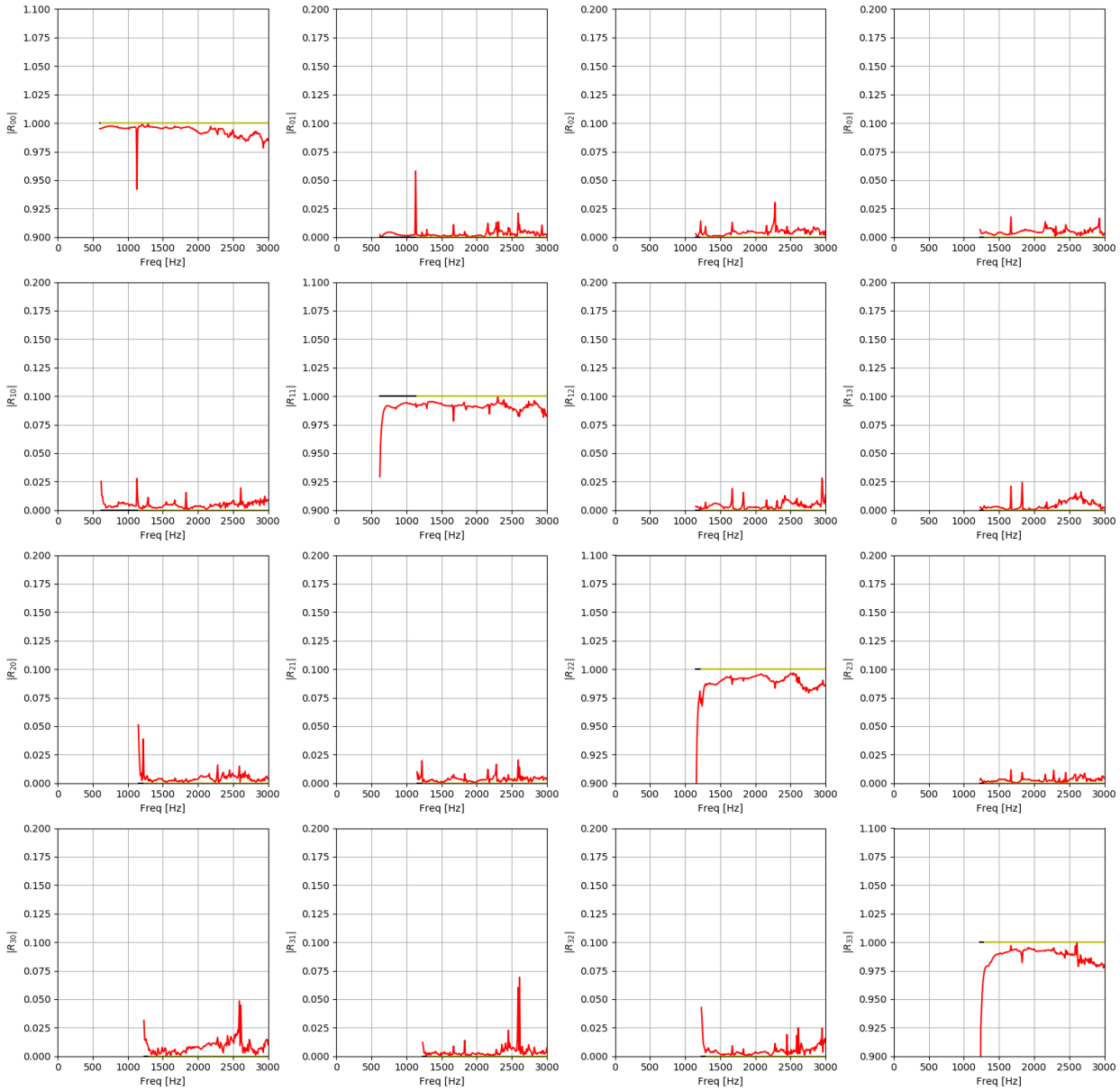

Fig. 3 First 16 coefficients of the 13x13 matrix of multimodal reflection coefficients of a rigid plate installed as boundary condition in the duct. The graphs on the diagonal represent the reflection of each mode to itself (and should thus be close to one), whereas the other graphs represent the cross-mode transfer (and should be close to zero).

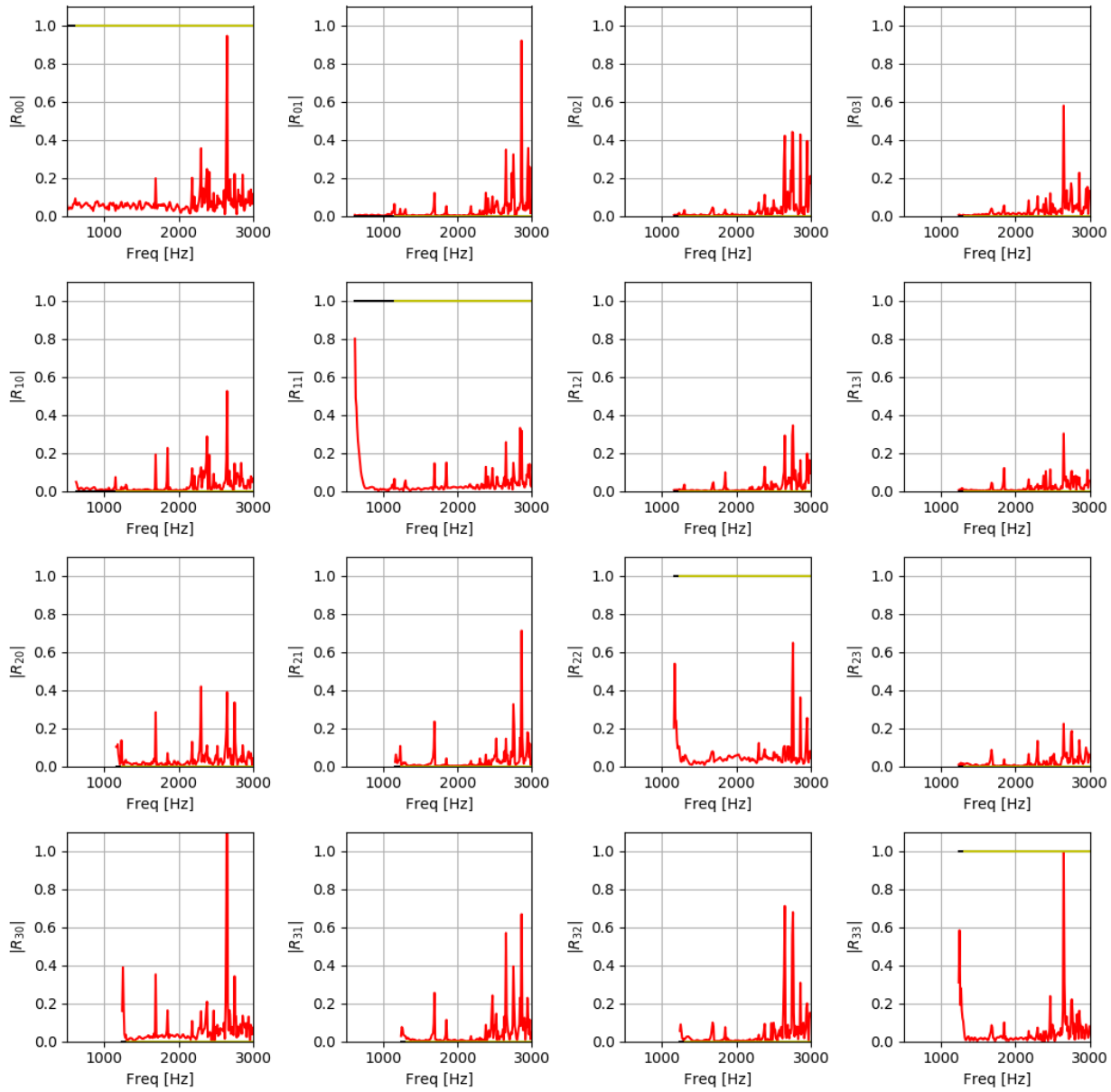

Fig. 4 First 16 coefficients of the 13x13 matrix of multimodal reflection coefficients measured for the anechoic termination.

B. Measurement functionalities

1. Forcing of duct modes independently

Some results of mode-by-mode excitations are presented here. The goal is to control the acoustic sources in such a way that the incident acoustic field contains only a particular mode. In Figure 5, the case without flow is presented. In this figure, the amplitude of the modes measured in the duct when the single modes were required are plotted in the left two columns. The right column is the emergence of the desired mode compared to the other (undesired) modes in the duct. In Figure 6 and Figure 7, the same results are presented for M = 0.4 for the upstream and downstream cases. Here, the amplitude of the controlled mode is set to 130 dB. Similar results were obtained without quality loss with other command amplitudes, up to 145 dB.

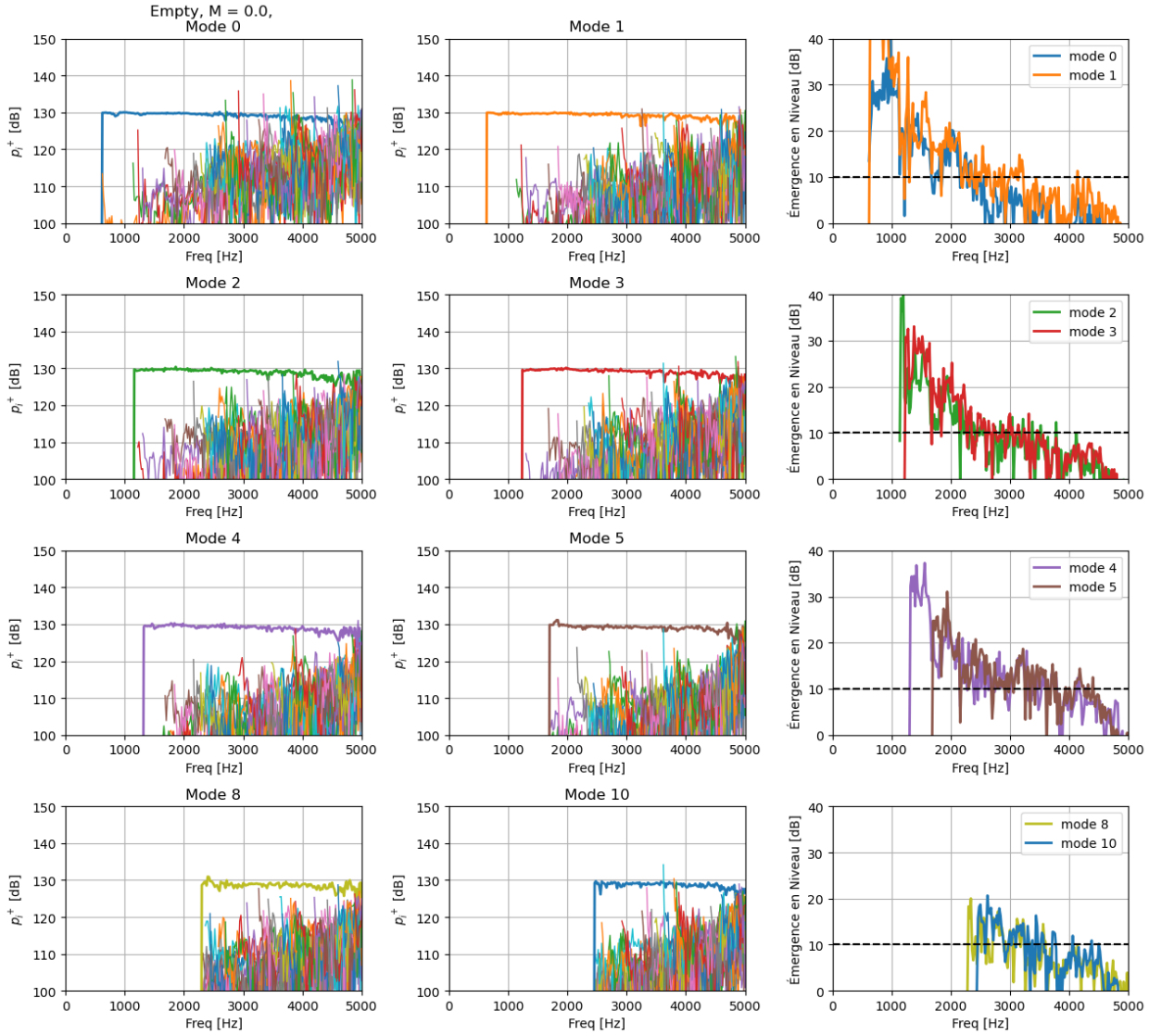

Fig. 5 Amplitude of the modes present in the upstream duct when each mode is excited independently (left two columns) without flow. The amplitude of the desired mode is plotted with a thick line. The figures on the right show the emergence of the desired mode compared to the other modes during each test. The SPL target was set to 130 dB for the desired mode.

In practice, the selectivity of the method depends on the quality of the previously identified transfer matrix used to compute the signals sent to the sources, and on the signal-to-noise ratio during the measurements, which is of course less favorable at high flow velocities. However, we notice in these figures that it is possible to excite any chosen single mode and to obtain an emergence greater than 10 dB for a large number of frequencies, even in presence of flow. Note that the frequency range for which the control is efficient is slightly reduced in the case of the downstream excitation.

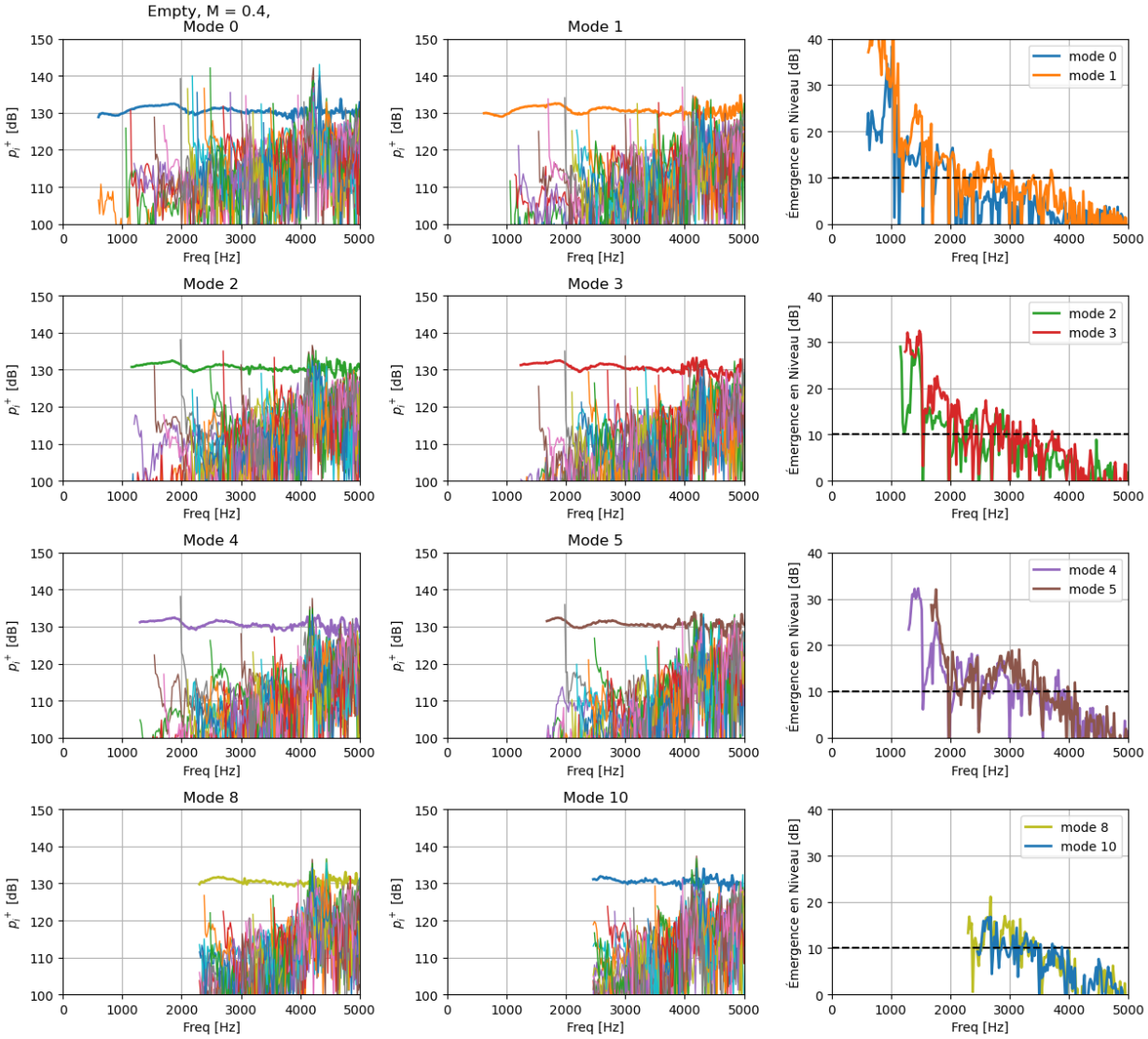

Fig. 6 Amplitude of the modes present in the upstream duct when each mode is excited independently (left two columns) at M = 0.4. The amplitude of the desired mode is plotted with a thick line. The figures on the right show the emergence of the desired mode compared to the other modes during each test. The SPL target was set to 130 dB for the desired mode.

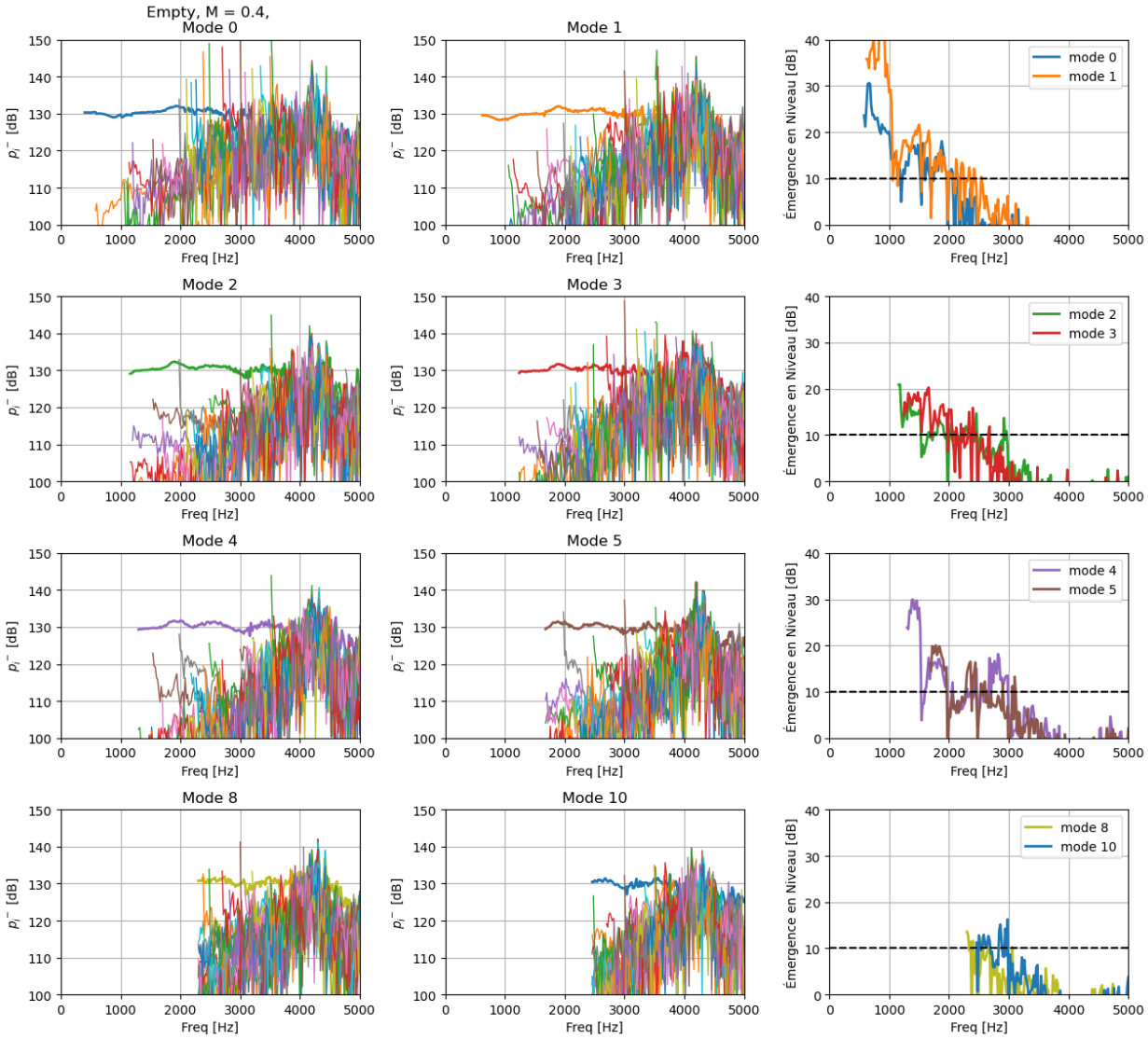

Fig. 7 Amplitude of the modes present in the downstream duct when each mode is excited independently (left two columns) at M = 0.4. The amplitude of the desired mode is plotted with a thick line. The figures on the right show the emergence of the desired mode compared to the other modes during each test. The SPL target was set at 130 dB for the desired mode.

2. Scattering matrix measurements

Results of scattering measurements are presented in the following. Two cases are considered: the test section without sample (which makes it a straight empty duct) and with a sample (SDOF with a thickness $\simeq$ 33 mm). The full scattering matrices have been measured using the multi-source methodology discussed in Section III-C. Here, only the multi-modal transmission matrices are presented. For example, the transmission matrices measured without flow are presented in Figure 8. In the case without sample (blue lines), we observe that the transmission coefficients are close to one on the diagonal, and close to zero otherwise. The deviation from the canonical values is larger at high frequencies due to the absence of attenuation in the wavenumber used for solving the system. Furthermore, beyond 4300 Hz, the low conditioning of the propagation matrix is not compensated by the over-determination (the number of modes becomes close to the number of microphones), which offers less accurate measurements, probably explains the drop of $T_{ii}^{\pm}$. In the case with sample (orange lines), the diagonal transmission coefficients deviate strongly from unity at certain frequencies. The ratio between the two curves (with and without sample) provide the Insertion Loss of each mode in itself. Furthermore, the transmission matrix is not diagonal any more, as the scattering by the sample transfers energy between the modes. To calculate the complete Insertion Loss for a particular incident mode, one should use all the coefficients in the corresponding column of the transmission matrix. As in the plane-wave case (with only one propagating mode), we can verify that the transmission matrices $\mathbf{T}^{+}$ and $\mathbf{T}^{-}$ are identical due to reciprocity.

Results with flow ($M = 0.2$) are presented in Figure 9. In this case, the reciprocity is broken and the matrices $\mathbf{T}^{+}$ and $\mathbf{T}^{-}$ are not identical. As for the case without flow, the Insertion Losses for each mode into itself can be evaluated from the diagonal coefficients, and the complete Insertion Loss for each incident mode should be evaluated from all the coefficients of the corresponding columns of the transmission matrices to account for the scattering by the sample.

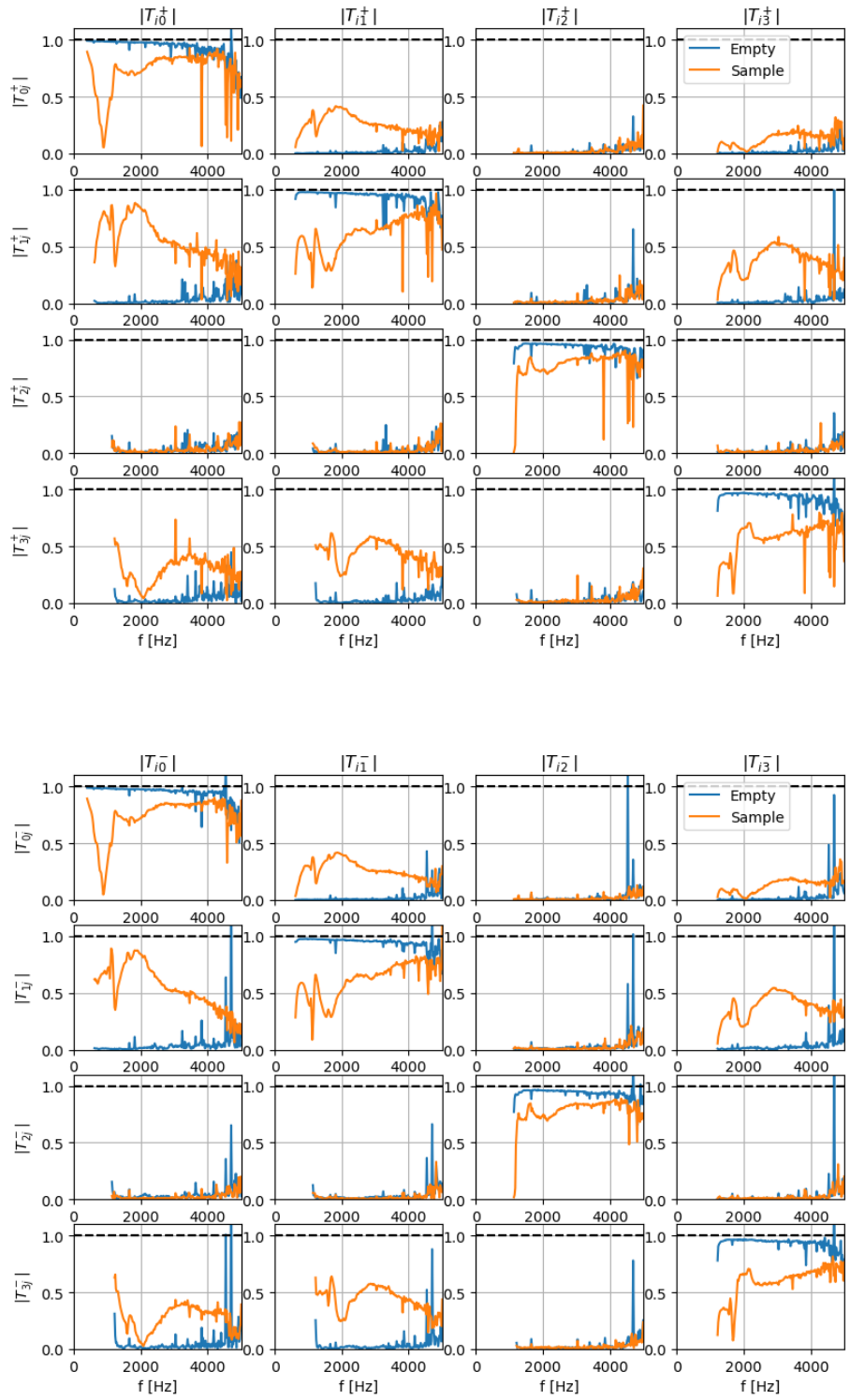

Fig. 8 First coefficients of the transmission matrices measured without flow for the empty duct (blue lines) and with a liner sample (orange lines). The upper group of 16 sub-figures show the coefficients of the transmission matrix $\mathbf{T}^{+}$ from upstream to downstream and the lower group of 16 sub-figures show the coefficients of the transmission matrix $\mathbf{T}^{-}$ from downstream to upstream. In both cases, only the coefficients for the first 4 modes are shown here.

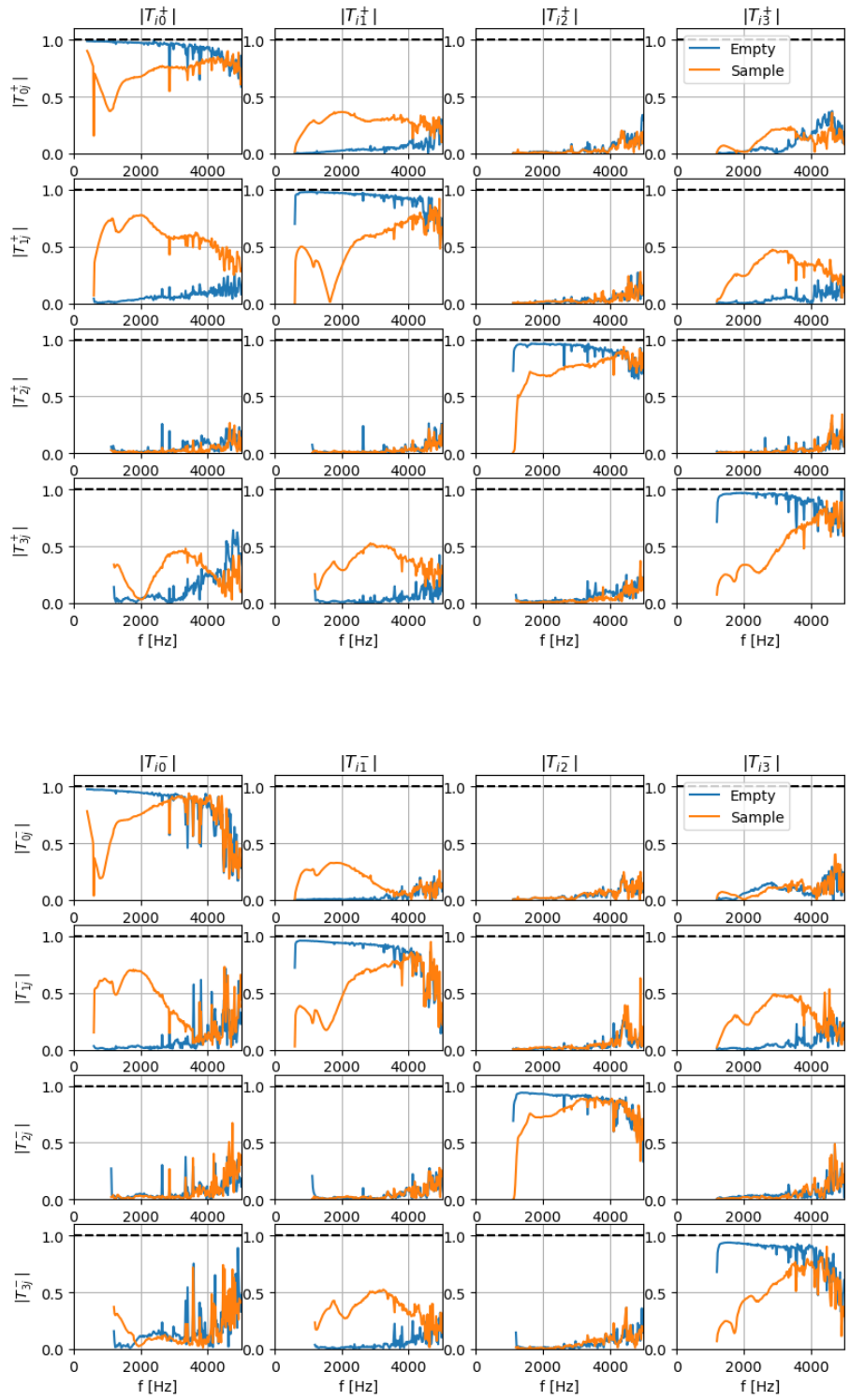

Fig. 9 First coefficients of the transmission matrices measured at M=0.2 for the empty duct (blue lines) and with a liner sample (orange lines). The upper group of 16 sub-figures show the coefficients of the transmission matrix T^+ from upstream to downstream and the lower group of 16 sub-figures show the coefficients of the transmission matrix T^- from downstream to upstream. In both cases, only the coefficients for the first 4 modes are shown here.

3. Insertion loss of a liner sample evaluated with broadband noise

The Insertion Losses measured without flow and at $M = 0.2$, $M = 0.4$ and $M = 0.6$ (for the same liner sample as above) with broadband noise between 400 Hz and 10kHz is plotted in Figure 10.

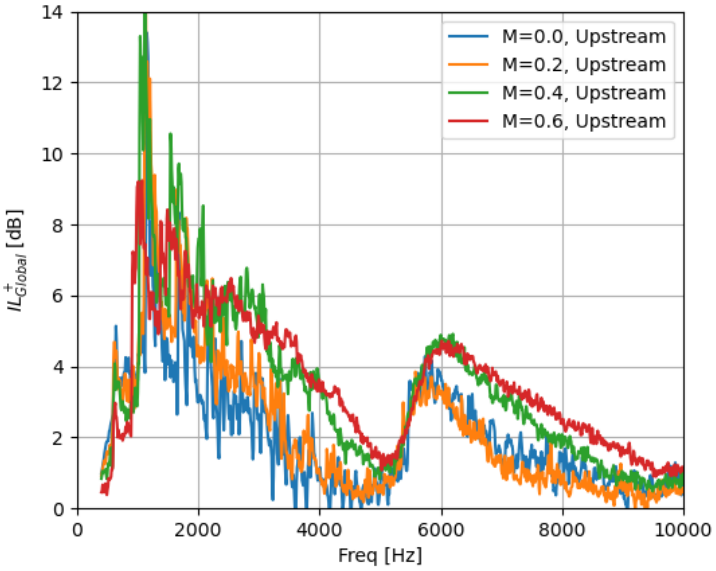

Fig. 10 Insertion Loss from upstream to downstream of a liner sample measured with broadband-noise excitation at different flow conditions.

V. Conclusions

A test-rig called "MAINE Flow », for Multimodal Acoustic ImpedaNce Eduction with Flow, has been developed and built in Le Mans. This facility allows to test liner samples under flow and acoustic conditions that are similar to what is found in aircraft engines. In particular, the acoustic scattering induced by the sample is quantified for mean Mach numbers up to 0.6 and for any given incident acoustic mode or combination of modes. Moreover, the amplitude of the controlled acoustic field can be set to 150 dB for broadband noise, and up to 145 dB (even slightly more without flow) for controlled modes.

In the present contribution, the modal decomposition and the scattering matrix estimation have been validated for canonical geometries such as a rigid plate and an anechoic termination. Then, a demonstration of the modal control in the test duct is provided. Last, examples of measurements of the scattering matrix and of the Insertion Loss for a typical SDOF liner are given.

Such developments will allow in a near future multi-modal characterization of liners to increase their TRL (Technology Readiness Level) in realistic flow- and acoustic conditions. Furthermore, the new facility and methods will allow advanced research works. In particular, further investigations will be undertaken on the interactions between the boundary layer above the liner and the acoustic field, in order to better understand the links between impedance and the acoustic waves propagation direction. Finally, the effects of the angle of arrival in presence of flow can also be studied thanks to the methods displayed and validated in the present paper.

References

[1] Golliard, J., Leroux, J.-C., Portier, E., Aurégan, Y., and Humbert, T., "Experimental facility for characterization of liners subjected to representative acoustical excitation and grazing flow," *Proceedings of the 25th AIAA/CEAS Aeroacoustics Conference, 2019, Delft, NL*, 2019.

[2] Renou, Y., and Aurégan, Y., "Failure of the Ingard-Myers boundary condition for a lined duct: An experimental investigation," *Journal of the Acoustical Society of America*, Vol. 130, No. 1, 2011, pp. 52–60.

[3] Weng, C., Schulz, A., Ronneberger, D., Enghardt, L., and Bake, F., "Impedance eduction in the presence of turbulent shear flow using the linearized Navier-Stokes equations," *Proceedings of the 23nd AIAA/CEAS Aeroacoustics Conference, 2017, Denvers, CO*, 2017.

[4] Roncen, R., Piot, E., Méry, F., Simon, F., Jones, M. G., and Nark, D. M., "Wavenumber-Based Impedance Eduction with a Shear Grazing Flow," *AIAA Journal*, Vol. 58, No. 7, 2020, pp. 3040–3050.

[5] Sitel, A., Ville, J.-M., and Foucart, F., "Multiload procedure to measure the acoustic scattering matrix of a duct discontinuity for higher order mode propagation conditions," *The Journal of the Acoustical Society of America*, Vol. 120, No. 5, 2006, pp. 2478–2490.

[6] Sack, S., Abom, M., Schram, C., and Kucukcoskun, K., "Generation and scattering of acoustic modes in ducts with flow," *"Proceedings of the 20th AIAA/CEAS Aeroacoustics Conference, Atlanta, GA*, 2014.

[7] Sitel, A., Ville, J.-M., and Foucart, F., "An Experimental Facility for Measurement of Acoustic Transmission Matrix and Acoustic Power Dissipation of Duct Discontinuity in Higher Order Modes Propagation Conditions," *Acta Acustica united with Acustica*, Vol. 89, No. 4, 2003, pp. 586–594.

[8] Bi, W., Pagneux, V., Lafarge, D., and Aurégan, Y., "Characteristics of penalty mode scattering by rigid splices in lined ducts," *The Journal of the Acoustical Society of America*, Vol. 121, No. 3, 2007, pp. 1303–1312.

[9] Aurégan, Y., Leroux, M., and Pagneux, V., "Measurement of liner impedance with flow by an inverse method," *10th AIAA/CEAS Aeroacoustics Conference*, 2004, p. 2838.